

Demonstration Scheme for a Laser-Plasma-Driven Free-Electron Laser

A. R. Maier,^{1,2,3,*} A. Meseck,⁴ S. Reiche,⁵ C. B. Schroeder,⁶ T. Seggebrock,³ and F. Grüner^{1,2,3}

¹*Center for Free-Electron Laser Science, Notkestrasse 85, 22607 Hamburg, Germany*

²*Institut für Experimentalphysik, Universität Hamburg, 22607 Hamburg, Germany*

³*Department für Physik, Ludwig-Maximilians Universität, 85748 Garching, Germany*

⁴*Helmholtz-Zentrum Berlin für Materialien und Energie, 14109 Berlin, Germany*

⁵*Paul Scherrer Institut, 5232 Villigen PSI, Switzerland*

⁶*Lawrence Berkeley National Laboratory, Berkeley, California 94720, USA*

(Received 11 May 2012; published 27 September 2012)

Laser-plasma accelerators are prominent candidates for driving next-generation compact light sources, promising high-brightness, few-femtosecond x-ray pulses intrinsically synchronized to an optical laser, and thus are ideally suited for pump-probe experiments with femtosecond resolution. So far, the large spectral width of laser-plasma-driven beams has been preventing a successful free-electron laser (FEL) demonstration using such sources. In this paper, we study the application of an optimized undulator design and bunch decompression to large-energy-spread beams in order to permit FEL amplification. Numerically, we show a proof-of-principle scenario to demonstrate FEL gain in the vacuum ultraviolet range with electron beams from laser-plasma accelerators as *currently* available in experiments.

DOI: [10.1103/PhysRevX.2.031019](https://doi.org/10.1103/PhysRevX.2.031019)

Subject Areas: Photonics, Plasma Physics

I. INTRODUCTION

Envisioning a compact and affordable electron accelerator on a laboratory scale, laser-wakefield accelerators (LWFA) [1,2] are attracting increasing interest, especially as candidates for driving next-generation free-electron lasers (FELs) [3–5]. Without doubt, increased availability of such a compact, high-brightness x-ray source, featuring a few-femtosecond (fs) pulse length combined with intrinsic few-fs temporal synchronization to an optical laser beam, would have enormous impact on many scientific disciplines [6].

Insufficient electron-beam quality, foremost the electron-beam energy spread, which is typically on the percent level for current LWFA-generated beams [7–9], is usually considered the greatest obstacle in realizing a laser-plasma-driven FEL, and so far no laser-plasma-based FEL has been demonstrated.

However, a consequent adjustment of the FEL setup for increased energy-spread acceptance, using large undulator parameters and longitudinal bunch decompression, can permit FEL amplification even for beams of relatively large spectral width. Based on recent novel diagnostic experiments, which characterized the typical LWFA emittance [9–12], bunch length [13,14], and slice-energy spread [15], we demonstrate the application of an optimized undulator and longitudinal bunch decompression to currently available laser-plasma-generated beams. We

conclude with a start-to-end simulation of a proof-of-principle experiment, which solely focuses on demonstrating detectable FEL gain well above the spontaneous emission background using a laboratory-size, 2-m-long undulator. We find that laser-plasma beams similar to those currently available may be sufficient to generate experimentally detectable FEL gain.

Knowledge of the slice-energy spread is a crucial parameter and still difficult to access experimentally and thus imposes an uncertainty on the experiment design. Therefore, after optimizing the undulator design (Sec. II) and defining parameters of a *typical* electron bunch, where the electron-beam energy spread $\hat{\sigma}_\gamma \equiv \sigma_\gamma/\gamma$ and bunch charge Q are free parameters, we study different scenarios to determine the minimum requirements on the electron beam for demonstrating FEL gain: First, we assume an uncorrelated energy spread (Sec. III) in our studies, followed by the assumption of a correlated energy spread (Sec. IV) as indicated by recent experiments. Adding a simple magnetic chicane for bunch decompression can further increase the performance of the FEL (Sec. V), and we find that experimentally demonstrated laser-plasma electron beams could show FEL gain.

II. UNDULATOR DESIGN

A highly relativistic electron beam of normalized energy γ , propagating through an undulator characterized by the dimensionless parameter $K \approx 0.93\lambda_u[\text{cm}] \times B[\text{T}]$, with λ_u the undulator period and B the on-axis magnetic field, emits on-axis radiation of wavelength $\lambda = \lambda_u(1 + K^2/2)/(2\gamma^2)$. For high-electron-density beams, the emitted radiation field couples to the electron bunch, causing an energy modulation and consequently a density modulation (microbunching) of period λ along the bunch, leading to

*andreas.maier@desy.de

Published by the American Physical Society under the terms of the [Creative Commons Attribution 3.0 License](https://creativecommons.org/licenses/by/3.0/). Further distribution of this work must maintain attribution to the author(s) and the published article's title, journal citation, and DOI.

coherent emission of radiation with radiated pulse energies many orders of magnitude above the purely spontaneous emission. The dimensionless Pierce parameter ρ [16],

$$\rho = \frac{1}{4\gamma} \left(\frac{I}{I_A} \frac{K^2 [JJ]^2 \lambda_u^2}{\pi^2 \sigma_x^2} \right)^{1/3},$$

with I the electron-beam peak current, $I_A \approx 17$ kA the nonrelativistic Alfvén current, σ_x the mean rms transverse beam size, the field-coupling defined as $[JJ] = J_0(Y) - J_1(Y)$, J_0 and J_1 Bessel functions, and $Y = K^2/(4 + 2K^2)$, scales the 1D FEL gain length $L_g = \lambda_u/4\pi\sqrt{3}\rho$, which is the e-folding length of the radiated power. At the same time, it also limits the acceptable beam energy spread to

$$\hat{\sigma}_\gamma \ll \rho,$$

preventing velocity differences to wash out the microbunching buildup. Meeting this requirement is a challenge for laser-plasma-driven beams, with experimentally demonstrated energy spreads usually on the percent level [7–9].

As a consequence, the first and foremost design goal in the presented FEL demonstration schemes is to maximize the Pierce parameter in order to increase the energy-spread acceptance of the FEL process to the range of currently available LWFA beams. Therefore, we optimize the undulator design, defined by K , λ_u , and the undulator gap g , thus tuning ρ independently from electron-bunch properties, and obtain an undulator generally suitable for maximum energy-spread acceptance.

For short gain lengths, the L_g scaling requires small undulator periods (assuming a fixed ρ), while the latter is maximized by large λ_u and K values. With the on-axis undulator field approximated by $B = a \exp(bg/\lambda_u + cg^2/\lambda_u^2)$, with material- and undulator-design-dependent fit parameters a , b , and c [17], we can set K almost independently from λ_u by varying the undulator gap. Choosing g in the few-mm range enables high K values at reasonable, small undulator periods, with parameters eventually limited by technical constraints: For a hybrid planar vanadium permendur undulator, $a = 3.694$ T, $b = -5.068$, and $c = 1.520$, which is valid for $0.1 < g/\lambda_u < 1$ [17], whereas for recently developed cryocooled undulator designs [18,19], $a = 4.023$ T, $b = -3.117$, and $c = 2.012$, for $\lambda_u = 15$ mm, are possible [20].

Balancing the K -dependent Pierce parameter ρ and the λ_u dependent gain length L_g , while minimizing λ_u and maximizing the undulator gap, we select an undulator design of $K = 3.3$, $\lambda_u = 15$ mm, $g = 2.5$ mm. The gap is thus slightly smaller than theoretically possible from the cryofit coefficients [20] and allows for a relaxed pole design of the individual undulator periods, adding a safety margin to the undulator design. We choose an undulator length of 2 m to allow a compact setup and avoid refocusing optics between undulator modules. For optimized FEL performance with a simple planar undulator design, we match the electron-beam optic to the natural focusing of

the undulator, while in the undulator wiggle plane we minimize the averaged β function.

Relatively small mm-scale undulator gaps combined with kA peak currents can cause significant resistive wall and surface roughness wakefield effects, which hinder the FEL process. Therefore, we include longitudinal resistive wall wakefields in all our calculations. Surface roughness wakefields are not included in the calculations, as we consider them negligible, assuming an in-vacuum undulator with foil-covered magnet poles. In general, for laser-plasma-driven FELs, the bunch length is typically smaller than the characteristic single-electron wakefield length $s_0 = (cg^2/8\pi\sigma)^{1/3}$, usually on the order of several microns [21], where c denotes the speed of light and σ is the conductivity of the boundary surface (beam pipe). For such electron-bunch lengths, with $\sigma_z \ll s_0$, the single-electron wakefields add coherently, causing a *linear* energy chirp along the electron bunch, which can, in principle, be compensated by tapering the undulator [22].

For ultrahigh current beams also, space-charge effects can drive the buildup of a linear energy chirp along the bunch. However, as shown in [23], there is an upper limit to the dynamically evolving energy chirp $\alpha \equiv d\gamma/\langle\gamma\rangle d\zeta$, with ζ the longitudinal bunch coordinate. The evolution of α is dependent on the combination of bunch charge and energy, where the latter dilates the effects in time such that they become negligible over the propagation length through the experimental setup. With the beam parameters defined in Sec. III we thus ignore space-charge-driven energy chirps.

III. UNCORRELATED ENERGY SPREAD

Accessing the phase-space information of an electron bunch on the fs scale [13,14] is experimentally challenging and so far no complete 6D phase-space characterization using a single laser-plasma-generated bunch has been performed. However, as recent diagnostic experiments [10–15] agree with simulations and general theoretical predictions [2], the properties measured in these experiments do set a parameter range and allow us to define a *typical* electron bunch that can be expected from a laser-plasma accelerator, operating at a few 10^{18} cm⁻³ plasma density and using a few tens of terawatt laser power. In order to base our studies on experimentally verified data [10,13,14], we assume an electron bunch with a normalized transverse emittance of $\epsilon_{x,y} = 0.2$ mm mrad at a moderate normalized beam energy of $\gamma = 600$. Since different experiments report similar bunch lengths at different bunch charges [13,14], the bunch charge Q is chosen as a free parameter in our studies and we assume a Gaussian current profile of $\sigma_z = 0.5$ μ m, which is consistent with [13,14]. But even though we rely on a certain parameter set, the schemes presented in Secs. III, IV, and V are robust and can be easily adapted to a change in parameters if an

experimentally realized beam differs from these idealized parameters.

Based on our bunch parameters and using the undulator described in Sec. II, we perform FEL simulations with GENESIS [24], scanning Q and $\hat{\sigma}_\gamma$ in a range of $Q = 10\text{--}40$ pC, to determine the minimum bunch-charge and energy-spread combination required for FEL gain under the assumption of an uncorrelated energy spread. All FEL simulations throughout this work are calculated with the time-dependent mode of GENESIS. The electron-beam transport before the undulator is not included for the simulations in Sec. III and IV. We choose a maximum of $\hat{\sigma}_\gamma = 1\%$ to limit chromatic effects that would occur in the beam transport optic. Since currently available FEL codes are not able to correctly model the dynamic space-charge-driven debunching for ultrahigh currents [23,25], we limit our studies to $I < 10$ kA.

Figure 1 shows in a \log_{10} scale the total emitted power at the end of the 2-m-long undulator, normalized to the purely spontaneous emission. The spontaneous emission is obtained from a linear fit to the lethargy regime of the FEL power curve, which is calculated by GENESIS within a 100% bandwidth. Although the spontaneous power level at the undulator end is thereby slightly underestimated, the signal-to-noise ratio can be significantly improved by spectrally and angularly resolving the FEL power, employing the different spectral and angular dependencies of spontaneous and amplified radiation. Thus, the linear fit to the lethargy regime serves as a reasonable estimation of the expected spontaneous power. Each data point is averaged over a set of 10 runs with different shot-noise seeds.

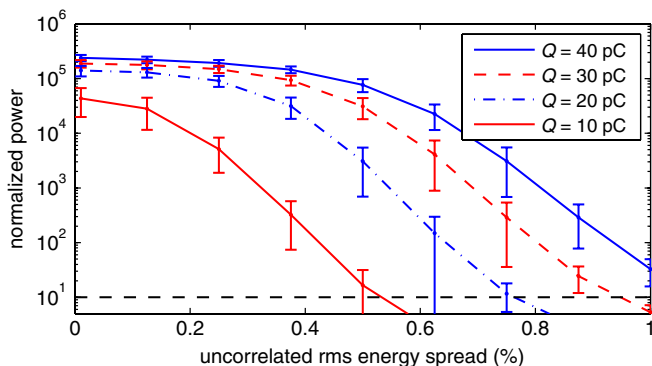


FIG. 1. Total emitted power (log scale) normalized to the spontaneous radiation level, scanning bunch charge, and rms energy spread in a range of $Q = 10\text{--}40$ pC, corresponding to beam currents $I = 2.4\text{--}9.6$ kA, Pierce parameters $\rho = 1.4\text{--}2.3\%$, and $\hat{\sigma}_\gamma \approx 0\text{--}1.0\%$, respectively. Data are obtained from time-dependent GENESIS simulations, with each data point averaged over 10 runs with different shot-noise seeds, and error bars marking the standard deviation of the fluctuation in shot-to-shot power. The black dashed line indicates an amplification by an order of magnitude above the spontaneous background. With the optimized undulator, FEL gain is possible even for very-large-energy-spread beams.

Resistive wall wakefield effects are included, assuming a flat aluminum beam pipe as an approximation to an in-vacuum undulator with foil-covered magnet poles. However, the relative wakefield-induced energy loss for the electron beam of $\gamma = 600$ is at a peak current of 9.6 kA, $Q = 40$ pC, below 0.2%/m, with less effect for smaller bunch charges, and is thus not the dominant effect. The figure illustrates that FEL gain could be shown even at an unusually high beam-energy spread of $\hat{\sigma}_\gamma = 1\%$, if the bunch charge of 40 pC, or 10 kA current, can be reached.

However, with a beam energy of $\gamma = 600$ the resonant wavelength $\lambda = 134$ nm is close to the assumed $\sigma_z = 0.5$ μm , and consequently it is important to consider the small bunch length of laser-plasma driven beams: As the radiation field outruns the electron bunch after a few wavelengths, the coupling between field and electrons is reduced, which attenuates the self-amplification of the FEL. A measure for this is to normalize the cooperation length L_c , defined as the radiation slippage length over one gain length, by the electron-bunch length. For $L_c/\sigma_z = L_g \lambda/\lambda_u \sigma_z \rightarrow 1$, the cooperation length is close to the bunch length, and as the emitted radiation field outruns the electron bunch, the FEL process is hindered by a reduced field-bunch interaction. Using a 3D FEL model, which assumes an infinite bunch length but includes diffraction, transverse beam size, and energy-spread effects (compare [26,27]), the calculated cooperation length for $Q = 40$ pC is in the range of $L_c = 0.3\text{--}0.6$ μm for $\hat{\sigma}_\gamma = 0\text{--}1\%$ and $L_c/\sigma_z \approx 1$, and thus just at the threshold of possible FEL gain. We will discuss a method to mitigate this effect in Sec. V.

A large K parameter increases the ratio L_c/σ_z , which reduces the effective radiation-beam interaction length. Although this effect will reduce the interaction length for the very short plasma-generated bunches, the K -dependent energy acceptance is the dominant scaling, as illustrated in

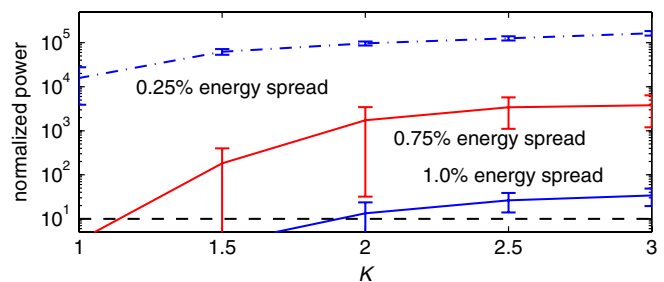


FIG. 2. Scan of the undulator parameter K by changing the undulator gap size, for an electron bunch of $Q = 40$ pC and different uncorrelated energy spreads. Error bars mark 1 standard deviation of the fluctuation in power originating from runs with different shot-noise seeds, with each data point averaged over 10 runs. Large undulator parameters are required to permit FEL gain for beams of broad spectral width. This dependency weakens as indicated by the flat curve for $\hat{\sigma}_\gamma = 0.25\%$ if the FEL is no longer dominated by the energy spread.

Fig. 2. Here, we select the parameter set from above ($Q = 40$ pC, $\hat{\sigma}_\gamma = 1\%$) that just allowed FEL amplification at very large energy spreads and then lower the undulator parameter to achieve shorter λ and thus longer interaction lengths. It is clearly shown that broad energy spectra require large K parameters for FEL gain and the longer interaction of the field and bunch cannot compensate the energy-spread-induced loss in gain. As expected, the power is only weakly dependent on K for smaller energy spreads. The figure also illustrates that the concepts discussed in this paper are not crucially dependent on reaching ultimate undulator performance, as the normalized power curves flatten for higher K .

As described in [28], with the bunch length σ_z on the same order as the FEL wavelength λ , the slowly varying amplitude approximation [16], usually implied to describe the FEL process, is not strictly fulfilled. However, as indicated in [28], this leads to an underestimation of the FEL gain, and therefore we consider the present simulations as a conservative estimation of the FEL process for extremely short electron bunches.

IV. ENERGY-CHIRPED ELECTRON BUNCH

Energy spectra currently measured in LWFA experiments are time integrated, as standard diagnostic methods are not able to resolve slice information for few-fs bunch lengths, and so far a correlation in the longitudinal energy distribution could not be directly verified. However, a recent experiment indirectly concludes the existence of a slice-energy spread much smaller than the measured integrated spectrum, through studying the long-range evolution of coherent optical transition radiation from LWFA beams [15]. This is also expected from LWFA theory: A spread in injection time loads different phases of the accelerating field, resulting in an energy chirp α along the bunch and eventually a broad time-integrated energy spectrum, while the slice-energy spread remains significantly smaller.

Following the measurements in [15], we assume in the remainder of this paper an electron bunch with a slice-energy spread of $\hat{\sigma}_{\gamma,s} \equiv \sigma_{\gamma,s}/\gamma = 0.5\%$, which requires a linear energy chirp of $\alpha = 1\%/\sigma_z$, to result in the same time-integrated energy spread of $\hat{\sigma}_\gamma = 1\%$ as in Sec. III. In principle, laser-plasma accelerators allow positive and negative chirps by terminating the acceleration before or after the dephasing, respectively [2]. Because of the asymmetry of the FEL detuning curve, we choose for all our studies a positive chirp with higher electron energies at the head of the bunch to achieve higher FEL gain. Again, we perform GENESIS simulations to study the effect of introducing an energy chirp to the bunch. As shown in Fig. 3, the bunch charge required to demonstrate FEL gain drops to $Q = 20$ pC for the same integrated energy spread of 1%, assuming $\hat{\sigma}_{\gamma,s} = 0.5\%$, and is less for smaller slice-energy spreads.

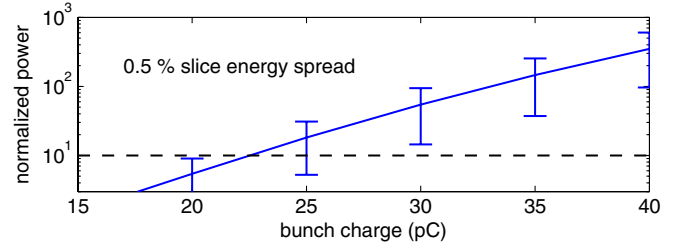


FIG. 3. Normalized power (log scale), for a chirped bunch, $\alpha = 1\%/\sigma_z$, with a slice-energy spread of $\hat{\sigma}_{\gamma,s} = 0.5\%$. About 20 pC in $\sigma_z = 0.5 \mu\text{m}$ are sufficient to demonstrate FEL gain.

For a small slice-energy spread, the *local* gain length is reduced, which enhances FEL amplification. On the global scale of the whole bunch, the resonance wavelength slightly changes along the bunch due to the energy chirp, but as the Pierce parameter is large, the radiation field can adopt to this variation, while slipping along the bunch. As we have shown, with the experiment-motivated assumption of a slice-energy spread, and for a regime where $L_c/\sigma_z \approx 1$, a demonstration FEL may work with a much smaller charge and higher energy spreads than one would conclude from measured time-integrated spectra and simple 1D estimations.

V. STRETCHING THE BUNCH

In Sec. III we find that the FEL amplification is reduced for wavelengths on the order of the electron-bunch length. An easy method to overcome this effect is to stretch the bunch in a magnetic chicane. Linearly stretching the bunch corresponds to a shear of the phase-space ellipsoid, which also linearly reduces the slice-energy spread and beam current. From the scaling of the pierce parameter $\rho \propto I^{1/3}$, one can expect that, for energy-spread-dominated regimes, the FEL performance is enhanced despite the drop in beam current. With the elongated interaction length of radiation and electron bunch, the FEL process is further promoted.

To demonstrate this effect, we linearly stretch the bunch length of the 20-pC chirped bunch case of Sec. IV in the range of $\sigma_z = 0.5\text{--}10.0 \mu\text{m}$, accordingly reduce the slice-energy spread, and perform a series of GENESIS simulations, which are shown in Fig. 4. Dots denote individual runs of different shot-noise seeds, the solid line represents the average normalized power of runs with identical σ_z , and the dashed lines mark 1 standard deviation of the fluctuation in radiated power. For $\sigma_z \approx 2 \mu\text{m}$, the normalized cooperation length is $L_c/\sigma_z \approx 0.5$ and enables FEL amplification, while the reduced slice-energy spread locally decreases the gain length and maintains the FEL process over a wide range of stretched bunch lengths, despite the drop in current. With significantly boosted FEL performance, less charge is required for detectable gain.

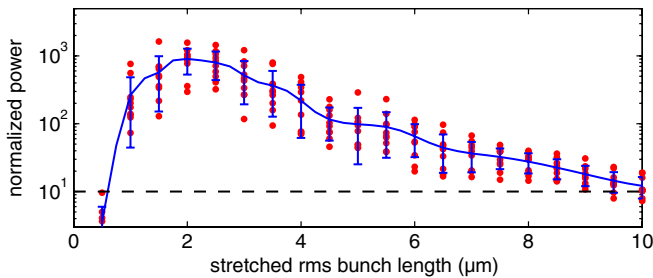


FIG. 4. Normalized power (log scale) for a stretched bunch of initially $\sigma_z = 0.5 \mu\text{m}$, 1% energy chirp over σ_z , and a slice-energy spread of $\hat{\sigma}_{\gamma,s} = 0.5\%$. The solid line is the average over 10 runs and the error bars mark 1 standard deviation of the shot-to-shot power fluctuation. FEL performance is significantly enhanced compared to the initial bunch length. Dots represent individual runs of different shot-noise seeds to illustrate the spread in power, which originates from the self-amplified spontaneous emission FEL starting from noise. The rms variation in pulse energy relates to the number of modes M in the FEL pulse and scales with $M^{-1/2}$ [33]. As the bunch length is comparably short, only a few modes are supported, leading to large shot-to-shot fluctuations.

These idealized calculations can be experimentally realized with a small magnetic chicane of longitudinal dispersion $R_{56} = 10\text{--}500 \mu\text{m}$. However, with beam currents on the kA level, coherent synchrotron radiation (CSR) effects in the chicane [29] need to be considered. Therefore, we include the electron-beam optic for the following simulations and perform complete start-to-end simulations using the particle tracking code ELEGANT [30], which includes a 1D model of CSR effects, to generate more realistic input files for subsequent GENESIS runs.

Starting at the plasma exit, we focus the electron bunch, using a triplet of permanent magnet quadrupoles [31], through a simple four-dipole chicane. As expected, CSR effects cause a slight, current-dependent emittance increase, mainly caused by a small transverse offset and shear of the beam, which can be partially corrected with appropriate steering elements.

We steadily lower the electron-beam charge starting from 20 pC. At $Q = 10$ pC and a stretched bunch length of $\sigma_z = 2.5 \mu\text{m}$, the radiated power is, on average, a factor of 5 above the spontaneous radiation level, which we consider as the detection threshold: For purely spontaneous emission, the bunch charge correlates linearly to the radiated power. With the onset of the nonlinear FEL process, the radiated power starts to vary dramatically for different shot-noise seeds, even for identical bunch charges. A cross correlation between bunch charge and shot-to-shot variation in photon pulse energy, allows then for an easy verification of FEL amplification.

Ultimately, we find that the FEL process can even be maintained for charges as low as 5 pC if we apply a linear taper to the undulator. In Fig. 5, we stretch a 5-pC bunch to $\sigma_z = 2.5 \mu\text{m}$ and vary the linear undulator taper, defined

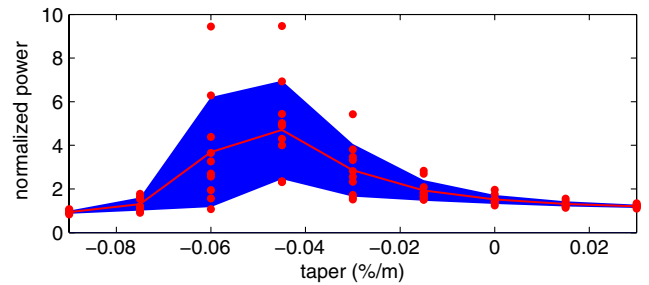


FIG. 5. Normalized power (linear scale) for a stretched $\sigma_z = 2.5 \mu\text{m}$, $Q = 5$ pC bunch, for a varying linear undulator taper. As before, dots mark individual runs and the solid line is the average over different shot-noise seeds. The blue area indicates 1 standard deviation of the spread in power.

as $K_{\text{enter}} = (1 - \delta)K_{\text{exit}}$, to maintain the resonant wavelength along the bunch. At the optimum taper [22], $\delta = 4.42\%/m$, the average signal is again a factor of 5 above the spontaneous background.

We cross-check the 1D CSR simulations with the fully 3D code CSRTRACK [32]. For bunch charges at the 20-pC level, the normalized transverse slice emittance increases so that it is approximately equal to 1 mmrad, and, as expected, hinders the FEL gain through a reduced current density in the undulator. However, 3D simulations also confirm a minimal emittance increase for the 5-pC bunch, still small enough to enable detectable FEL gain.

VI. CONCLUSIONS

Compared to other designs for laser-plasma-driven FELs [3–5], which require energy spreads similar to those from conventional accelerators, we have discussed in this paper the application of high- K undulators and longitudinal bunch decompression to enable FEL amplification with unusually high energy spreads, as available today from laser-plasma accelerators. Note that, in principle, these concepts can be applied to any large-energy-spread beam, independent of the source. A critical parameter in our concept is the undulator optimized for large undulator parameters to increase energy-spread acceptance, permitting FEL amplification at an unprecedented large energy spread of 1% with approximately 10 kA beam current. Nonetheless, undulators not reaching ultimate performance can be largely tolerated.

In the case of laser-plasma accelerators, it is expected that the measured energy spectrum is the result of a chirped bunch of a small slice-energy spread. For these parameters, the beam current required for FEL gain can be significantly reduced. For both scenarios, correlated and uncorrelated energy spreads, we discussed the limit on the bunch charge necessary for FEL gain.

However, for laser-plasma accelerators, the K -dependent FEL wavelengths on the order of the ultra-short electron-bunch lengths reduce the interaction length

of the radiation field with the electron bunch, which is the dominant degrading effect for FEL performance in this regime. By using a magnetic chicane to decompress the electron bunch, this effect can be compensated and the charge required for demonstrating FEL gain is reduced. This method is even independent of the assumption of a slice-energy spread, as with a slightly increased decompression factor an appropriate slice-energy spread can be introduced to an initially completely uncorrelated beam.

We have shown, using start-to-end simulations, that FEL gain could be demonstrated with a time-integrated energy spread of 1% rms and a bunch charge of only 5 pC by employing a high- K undulator and bunch decompression. The FEL wavelength in this setup is $\lambda = 134$ nm at an electron-beam energy of 300 MeV. These electron-beam parameters are similar to experimentally demonstrated beams.

Independent of specific electron-beam parameters, the scenarios presented in this work are generally valid and can easily be adapted to a concrete experimental setup. By consequently optimizing the undulator design and using simple electron-beam optics, a FEL demonstration experiment with today's laser-plasma driven electron beams seems to be possible.

ACKNOWLEDGMENTS

This work has been supported by the DFG Excellence Cluster Munich-Centre for Advanced Photonics (MAP). A. R. M. acknowledges financial support from the ESF SILMI network. C. B. S. acknowledges support from the Director, Office of Science, of the U.S. DOE under Contract No. DE-AC02-05CH11231.

-
- [1] T. Tajima and J. M. Dawson, *Laser Electron Accelerator*, *Phys. Rev. Lett.* **43**, 267 (1979).
 - [2] E. Esarey, C. B. Schroeder, and W. P. Leemans, *Physics of Laser-Driven Plasma-Based Electron Accelerators*, *Rev. Mod. Phys.* **81**, 1229 (2009).
 - [3] D. Habs, F. Grüner, U. Schramm, P. Thirolf, M. Sewtz, and S. Becker, *Design Considerations for Converting Laser-Accelerated Electron Beams into Brilliant X-Ray, Gamma-Ray and Neutron-Beams*, *AIP Conf. Proc.* **802**, 6 (2005).
 - [4] F. Grüner, S. Becker, U. Schramm, T. Eichner, M. Fuchs, R. Weingartner, D. Habs, J. Meyer-ter Vehn, M. Geissler, M. Ferrario, L. Serafini, B. van der Geer, H. Backe, W. Lauth, and S. Reiche, *Design Considerations for Table-Top, Laser-Based VUV and X-Ray Free Electron Lasers*, *Appl. Phys. B* **86**, 431 (2007).
 - [5] C. B. Schroeder, W. M. Fawley, F. Grüner, M. Bakeman, K. Nakamura, K. E. Robinson, Cs. Toth, E. Esarey, and W. P. Leemans, *Free-Electron Laser Driven by the LBNL Laser-Plasma Accelerator*, *AIP Conf. Proc.* **1086**, 637 (2009).
 - [6] K. Nakajima, *Compact X-Ray Sources: Towards a Tabletop Free-Electron Laser*, *Nature Phys.* **4**, 92 (2008).
 - [7] C. Rechatin, J. Faure, A. Ben-Ismaïl, J. Lim, R. Fitour, A. Specka, H. Videau, A. Tafzi, F. Burgy, and V. Malka, *Controlling the Phase-Space Volume of Injected Electrons in a Laser-Plasma Accelerator*, *Phys. Rev. Lett.* **102**, 164801 (2009).
 - [8] W. P. Leemans, B. Nagler, A. J. Gonsalves, Cs. Tóth, K. Nakamura, C. G. R. Geddes, E. Esarey, C. B. Schroeder, and S. M. Hooker, *GeV Electron Beams from a Centimetre-Scale Accelerator*, *Nature Phys.* **2**, 696 (2006).
 - [9] E. Brunetti, R. P. Shanks, G. G. Manahan, M. R. Islam, B. Ersfeld, M. P. Anania, S. Cipiccia, R. C. Issac, G. Raj, G. Vieux, G. H. Welsh, S. M. Wiggins, and D. A. Jaroszynski, *Low Emittance, High Brilliance Relativistic Electron Beams from a Laser-Plasma Accelerator*, *Phys. Rev. Lett.* **105**, 215007 (2010).
 - [10] R. Weingartner, S. Raith, A. Popp, S. Chou, J. Wenz, K. Khrennikov, M. Heigoldt, A. R. Maier, N. Kajumba, M. Fuchs, B. Zeitler, F. Krausz, S. Karsch, and F. Grüner, *Ultra-Low Emittance Electron Beams from a Laser-Wakefield Accelerator* (to be published).
 - [11] S. Kneip, C. McGuffey, J. L. Martins, M. S. Bloom, V. Chvykov, F. Dollar, R. Fonseca, S. Jolly, G. Kalintchenko, K. Krushelnick, A. Maksimchuk, S. P. D. Mangles, Z. Najmudin, C. A. J. Palmer, K. Ta Phuoc, W. Schumaker, L. O. Silva, J. Vieira, V. Yanovsky, and A. G. R. Thomas, *Characterization of Transverse Beam Emittance of Electrons from a Laser-Plasma Wakefield Accelerator in the Bubble Regime Using Betatron X-Ray Radiation*, *Phys. Rev. ST Accel. Beams* **15**, 021302 (2012).
 - [12] S. M. Wiggins, R. C. Issac, G. H. Welsh, E. Brunetti, R. P. Shanks, M. P. Anania, S. Cipiccia, G. G. Manahan, C. Aniculaesei, B. Ersfeld, M. R. Islam, R. T. L. Burgess, G. Vieux, W. A. Gillespie, A. M. MacLeod, S. B. van der Geer, M. J. de Loos, and D. A. Jaroszynski, *High Quality Electron Beams from a Laser Wakefield Accelerator*, *Plasma Phys. Controlled Fusion* **52**, 124032 (2010).
 - [13] A. Buck, M. Nicolai, K. Schmid, C. M. S. Sears, A. Sävert, J. M. Mikhailova, F. Krausz, M. C. Kaluza, and L. Veisz, *Real-Time Observation of Laser-Driven Electron Acceleration*, *Nature Phys.* **7**, 543 (2011).
 - [14] O. Lundh, J. Lim, C. Rechatin, L. Ammoura, A. Ben-Ismaïl, X. Davoine, G. Gallot, J.-P. Goddet, E. Lefebvre, V. Malka, and J. Faure, *Few Femtosecond, Few Kiloampere Electron Bunch Produced by a Laser-Plasma Accelerator*, *Nature Phys.* **7**, 219 (2011).
 - [15] C. Lin, J. van Tilborg, K. Nakamura, A. J. Gonsalves, N. H. Matlis, T. Sokollik, S. Shiraishi, J. Osterhoff, C. Benedetti, C. B. Schroeder, Cs. Tóth, E. Esarey, and W. P. Leemans, *Long-Range Persistence of Femtosecond Modulations on Laser-Plasma-Accelerated Electron Beams*, *Phys. Rev. Lett.* **108**, 094801 (2012).
 - [16] R. Bonifacio, C. Pellegrini, and L. M. Narducci, *Collective Instabilities and High-Gain Regime in a Free Electron Laser*, *Opt. Commun.* **50**, 373 (1984).
 - [17] P. Elleaume, J. Chavanne, and B. Faatz, *Design Considerations for a 1 Å SASE Undulator*, *Nucl. Instrum. Methods Phys. Res., Sect. A* **455**, 503 (2000).
 - [18] J. Bahrtdt, H.-J. Baecker, M. Dirsat, W. Frentrup, A. Gaupp, D. Just, D. Pflückhahn, M. Scheer, B. Schulz, R. Weingartner, F. Grüner, and F. O'Shea, in *Proceedings of the IPAC'10 (JACoW, Geneva, 2010)*.

- [19] F.H. O'Shea, G. Marcus, J.B. Rosenzweig, M. Scheer, J. Bahrtdt, R. Weingartner, A. Gaupp, and F. Grüner, *Short Period, High Field Cryogenic Undulator for Extreme Performance X-Ray Free Electron Lasers*, *Phys. Rev. ST Accel. Beams* **13**, 070702 (2010).
- [20] J. Bahrtdt, in *Proceedings of 33rd International Free Electron Laser Conference* (JACoW, Geneva, 2011).
- [21] K.L.F. Bane and G. Stupakov, Report No. SLAC-PUB 10707, 2004.
- [22] E.L. Saldin, E.A. Schneidmiller, and M.V. Yurkov, *Self-Amplified Spontaneous Emission FEL with Energy-Chirped Electron Beam and its Application for Generation of Attosecond X-Ray Pulses*, *Phys. Rev. ST Accel. Beams* **9**, 050702 (2006).
- [23] F.J. Grüner, C.B. Schroeder, A.R. Maier, S. Becker, and J.M. Mikhailova, *Space-Charge Effects in Ultrahigh Current Electron Bunches Generated by Laser-Plasma Accelerators*, *Phys. Rev. ST Accel. Beams* **12**, 020701 (2009).
- [24] S. Reiche, *Genesis 1.3: A Fully 3D Time-Dependent FEL Simulation Code*, *Nucl. Instrum. Methods Phys. Res., Sect. A* **429**, 243 (1999).
- [25] W.M. Fawley and J.-L. Vay, in *Proceedings of 32nd International Free Electron Laser Conference* (JACoW, Geneva, 2010).
- [26] M. Xie, in *Proceedings of the 1995 Particle Accelerator Conference* (JACoW, Geneva, 1995).
- [27] M. Xie, *Exact and Variational Solutions of 3D Eigenmodes in High Gain FELs*, *Nucl. Instrum. Methods Phys. Res., Sect. A* **445**, 59 (2000).
- [28] C. Maroli, V. Petrillo, and M. Ferrario, *One-Dimensional Free-Electron Laser Equations without the Slowly Varying Envelope Approximation*, *Phys. Rev. ST Accel. Beams* **14**, 070703 (2011).
- [29] E.L. Saldin, E.A. Schneidmiller, and M.V. Yurkov, *On the Coherent Radiation of an Electron Bunch Moving in an Arc of a Circle*, *Nucl. Instrum. Methods Phys. Res., Sect. A* **398**, 373 (1997).
- [30] M. Borland, Advanced Photon Source Report No. LS-287, 2000.
- [31] T. Eichner, F. Grüner, S. Becker, M. Fuchs, D. Habs, R. Weingartner, U. Schramm, H. Backe, P. Kunz, and W. Lauth, *Miniature Magnetic Devices for Laser-Based, Table-Top Free-Electron Lasers*, *Phys. Rev. ST Accel. Beams* **10**, 082401 (2007).
- [32] M. Dohlus and T. Limberg, in *Proceedings of 26th International Free Electron Laser Conference* (JACoW, Geneva, 2004).
- [33] E.L. Saldin, E.A. Schneidmiller, and M.V. Yurkov, *The Physics of Free Electron Lasers* (Springer, New York, 1999).